The novel pushing gravity model and volcanic activity. Is alignment of planets with compact stars a possible cause of natural phenomena?

F Greco[1] **and I V Krasnyy**[2]

[1] Istituto Nazionale di Geofisica e Vulcanologia, Sezione di Catania, Osservatorio Etneo, Catania, Italy
[2] The State Navigation-Hydrographic Institute (GNINGI), Saint-Petersburg, Russia

E-mail: 9968348@gmail.com; filippo.greco@ingv.it

Abstract. We developed the model, and carried out its discussion at the PIRT-2021 conference, within the framework of the research topic "*External Forcing on Volcanoes and Volcanic Processes: Observations, Analysis and Implications*" announced by the journal "Frontiers in Earth Science" in October 2020. Besides other, external processes considered in this Research Topic included astronomical. In this study, in the category "*Hypothesis and Theory*", we investigate how changes in the position of large bodies of the Solar system can cause natural phenomena, associated with the movement of free masses, such as volcanism, earthquakes and landslides in the lithosphere, as well as various catastrophic events in the atmosphere and hydrosphere. The analysis has shown that the discovered phenomena of celestial bodies' alignments accompanying manifestations of natural phenomena require going beyond the standard cosmological model and clarify the fundamental mechanism of gravity. We propose the novel *Bidirectional Pushing Gravitation* model (BPG), which, in addition to application in Earth Sciences, may occur useful in Astrophysics, Cosmology and Gravitation research.

1. Research goals and methods

The influence at different temporal and spatial scales of external processes on various geological phenomena such as seismicity and volcanism is widely discussed in the scientific literature. Despite it is still debated if the action of external forces (e.g. tidal stress changes) as low as a few kPa may trigger and regulate some natural phenomena [7], the extraordinary cyclicity of some phenomena, suggest an external forcing, such as Earth tides or planetary alignment, may induce changes in the dynamical state of the volcano constituting the ultimate trigger that may lead an active volcano to erupt.

Our research had two major goals - ***a) to verify the existence of the mentioned celestial bodies' alignment phenomena*** and ***b) to suggest a plausible model*** for its explanation, specifically:

- Investigation of Etna volcanic manifestations in order to identify the possible influence of astronomical factors, caused by changes in the position of large celestial bodies of the Solar system. Analysing alignments of the large celestial bodies of Solar system – the seven planets, dwarf planets Pluto and Ceres, the Sun and the Moon relative to Earth observer, coinciding with a wide range of various high-energy natural phenomena in lithosphere, hydrosphere and atmosphere. Discovering the features of alignments and possible force effects on natural phenomena, i.e., the induction of transient gravitational disturbances causing movement of free masses, variation of non-tidal plumb line deviations caused by changes in the position of

celestial bodies. Confirmation, refute, or detailing of the popular hypothesis about the phenomenon existence in the extent necessary to build a computational model of the induced gravitational perturbations.

- Proposal of a reasonable mechanism for transmitting gravitational perturbations, caused by changes in the position of large celestial bodies of the Solar system, into the geosphere and a model, which allows, taking into account the identified features, precomputing such perturbations for use in various applications.

To select the time series of registered natural phenomena that are subject to subsequent detailed analysis using ephemeris models, we used various databases volcanic [25] and seismic [26] events, as well as individual mentions of other natural phenomena that have a time reference to the exact or approximate date of their manifestation, and the planetarium program. We employed specialized software for calculating ephemerides and angular separations between celestial bodies Alcyone [28], online services for verification, as well as Excel spreadsheets with the connection of the Swiss Ephemeris library [27] via VBA, as the main tool. The position of celestial bodies at small angular separations and their alignment along several lines in some cases were displayed in the desktop application of the 3D planetarium Solar System Scope [29]. At the time of each event or selected time step, we calculated 220 angular separations for 11 celestial bodies of the Solar System and 15 fixed stellar objects, according to the number of combinations. The spreadsheet allowed us to set the required threshold value (1-5°) of angular separation in order to filter out cases of alignment of celestial bodies along one line.

All the analyzed natural phenomena are associated with the movement of free masses in the geosphere. Data on Etna volcanism were subject to detailed analysis in order to identify the external influence of extraterrestrial factors. The subject for analysis in the lithosphere included large earthquakes, manifestations of volcanism, landslides, mudslides, as well as individual man-made disasters provoked by gravity, “moving stones”, and anomalous data from various geophysical observations. In the hydrosphere - floods, manifestations of extreme (rogue) waves in the ocean, tropical storms. In the atmosphere - hurricanes, storms, supercells, tornadoes, wind shear in clear weather.

We did not plan to conduct an in-depth statistical analysis of the alignment effect of celestial bodies that accompanies all the mentioned variety of natural phenomena on Earth, especially taking into account (as will be shown below) that this effect is a) just a necessary condition for such phenomena; b) in general, there is a time shift between alignment and the manifestation of natural phenomena with anticipation or with time lag. Interested researchers can independently use the tools mentioned in this report. This study is a preliminary stage, the purpose of which is to propose a computational model and a method of its parameterization for the pre-calculation of gravitational perturbations from extraterrestrial sources.

2. State of the art

According to generally accepted theories, the influence of planets on terrestrial phenomena is negligible, and is proportional to the gradient of the gravitational field strength, i.e. inversely proportional to the cube of the distance. With regard to the possible mechanism of the influence of extraterrestrial bodies on terrestrial phenomena, only tides are considered, the intensity of which both in the hydrosphere and in the lithosphere significantly decreases with the distance to the disturbing celestial bodies. In the theory of Earth tides, only the lunar and solar harmonic constants (M2, S2, K1, O1) are considered. The gravitational influence of other celestial bodies on tides, as well as on any other terrestrial processes, is considered insignificant.

Some short-lived but significant correlations have been reported between semi-diurnal tides and the frequency of aftershocks in some volcanic regions, such as Mammoth Lakes. The Moon, the Sun and other planets have impact on Earth in the form of perturbations (small changes) of the gravitational field. The relative magnitude of the influence is proportional to the mass of the object and inversely proportional to the third power of its distance from the Earth. The stresses created on Earth by an

extraterrestrial mass are proportional to the gradient of the gravitational field $\frac{dg(r)}{dr}$, and NOT the strength of the gravitational field $g(r)$.

$$g(r)=\frac{GMm}{r^2}, \text{ thus: } \frac{dg(r)}{dr}=-\frac{2g(r)}{r}=-\frac{2GMm}{r^3} \quad (1)$$

(From the University of California, Berkeley, with the participation of Gary Fuis).

Maurice Allais (1911-2010, French physicist and economist), discovered and investigated the effect of abnormal behavior of pendulums during solar eclipses, named after him [16]. The study of the anomalous behavior of pendulums during solar eclipses was continued by the followers of M. Allais, who also reported the instability of the manifestation of the effect during various eclipses.

Gravitational anomalies are reported during lunar eclipses [18]. Alexander Pugach (1940-2020, GAO of the Academy of Sciences and the National Academy of Sciences of Ukraine), registered the anomalous behavior of torsion scales of his own design ("torsind"), as well as pendulums during syzygies (i.e., during solar and lunar eclipses), during transit of Venus across the solar disk, and when Venus is covered by the Moon.

"Observations were made of the torsion balance and the behavior of the "torsind" at the moments of solar and lunar eclipses, the passage of Venus behind the solar disk, and the eclipse of Venus by the Moon. It is shown that in most cases, the reaction of the devices to these phenomena was either ahead of or behind the actually observed phenomenon" [17].

With the help of a high-precision Lacoste-Romberg gravimeter, continuous and accurate measurements were made during the total solar eclipse of March 9, 1997 in the Mohe region in northeastern China. The presence of two "valleys of gravitational anomalies" with an almost symmetrical decrease in gravity by about 6 ~ 7 microgals at the first and last contact is noted [20].

There are publications about the violation of the synchronization of atomic clocks during solar eclipses, as well as observations that did not confirm this effect [21].

Also, in the context of the proposed mechanism of action of gravitation, it should be mentioned that there are a number of studies and publications claiming that the plasma is pushed out by gravity [19].

A number of researchers report the registration of non-tidal variations of plumb line deviations on dates coinciding with the alignment of celestial bodies [22], [23].

3. The analysis results and conclusions for constructing a model of gravitational perturbations

3.1. Alignment of celestial bodies during natural phenomena occurs near astronomical conjunctions, or oppositions relative to other planets, or compact stars

Almost all the analyzed natural phenomena are associated with the alignment of celestial bodies relative to the observer (a geophysical object, moving masses in the geosphere) at small angular distances (less than 3-5°, see the histogram, Figure 3) from one or several lines connecting two or more celestial bodies with each other, or with some "special points " that repeat for different events on the celestial sphere. Alignment occurs in the forward direction, near astronomical conjunctions (as during solar eclipses), and also (and even more often) in the opposite direction, near astronomical oppositions (as during lunar eclipses).

3.2. Compact stars induce gravitational perturbations when aligned with celestial bodies

The subsequent analysis showed that in the mentioned "special points" on the celestial sphere there are located compact stars with a high density of matter: red dwarfs, white dwarfs, clusters including such stars, neutron stars, as well as other galaxies. Since most of the celestial bodies of the solar system move near the ecliptic plane, the identified "special points" are also grouped near the ecliptic plane. For the primary analysis, we have chosen 15 stellar objects close to the ecliptic plane, near which the solar system bodies are located at the moments of the natural events' manifestation (Table 1).

Table 1. Stellar objects close to the ecliptic plane.

Name	Type	Const.	RA	DEC	Mass, $M_\odot$	Radius	Distance
IC 358	lenticular galaxy	Tau	$04^h03^m42.9^s$	+19°53′42″			92,900,222 pc
M1	Crab Nebula, neutron star	Tau	$05^h34^m31.97^s$	+22°00′52.1″	1.4 - 2.0	10 km	2,000 pc
M35	open cluster	Gem	$06^h08^m54.0^s$	+24°20′00″	1,600	11 ly	1,186 pc
M44	open cluster	Cnc	$08^h\ 40.4^m$	19°59′	500–600	7.5 ly	160-187 pc
M80	globular cluster	Sco	$16^h17^m02.41^s$	−22°58′33.9″	5.02×10^5	48 ly	10.0 kpc
NGC 4697	elliptical galaxy	Vir	$12^h48^m35.9^s$	−05°48′03″	BH 1.3×10^8		38-50 Mly
QS-Vir	white dwarf and red dwarf binary	Vir	$13^h49^m52.0032^s$	−13°13′37.002″	0.78	0.011 $R_\odot$	50.1 pc
AR-Sco	white dwarf and red dwarf binary	Sco	$16^h21^m47.28^s$	−22°53′10.3″	WD 0.81-1.29 RD 0.28-0.45		116 pc
Wolf 28	Van Maanen star, white dwarf	Psc	$00^h49^m09.89841^s$	+05°23′18.9931″	0.67	0.0138 $R^\odot$	4.3152 pc
Nu²Sgr or NGC6717?	binary with WD globular cluster	Sgr	$18^h55^m07.14098^s$ $18^h\ 55^m\ 06.04^s$	−22°40′16.8185″ −22° 42′ 05.3″			84 pc 7.1 kpc
Ross 154	red dwarf	Sgr	$18^h49^m49.36216^s$	−23°50′10.4291″	0.17	0.24 $R^\odot$	2.94 pc
Wolf 359	red dwarf	Leo	$10^h56^m28.99^s$	+07°00′52.0″	0.09	0.16 $R^\odot$	2.409 pc
Ross 128	red dwarf	Vir	$11^h47^m44.3969^s$	+00°48′16.4049″	0.168	0.1967 $R^\odot$	3.3749 pc
Trappist-1	red dwarf	Aqr	$23^h06^m29.283^s$	−05°02′28.59″	0.0898	0.1192 $R^\odot$	12.43 pc
K2-72	red dwarf	Aqr	$22^h18^m29.27^s$	−09°36′44.6″	0.271365	0.330989 $R^\odot$	66.56 pc

3.3. The transfer of gravitational perturbations to geosphere occurs through the jerk (derivative of acceleration) with a lag, or ahead of the bodies' alignments

Gravitational perturbations from extra-terrestrial masses on Earth, in addition to the gradient of the gravitational field, are also caused by a change in the strength of the external gravitational field over time, i.e., the derivative of acceleration, kinematic jerk. Figure 1 shows, for example, graphs of accelerations and their derivatives relative to the centre of mass of the Earth, plotted from ephemeris data. The graph clearly shows the obvious fact of the shift of the jerk phase (derivative) relative to the acceleration (primitive). The alignment of the celestial bodies' corresponds to the extremes of perturbing accelerations, however, gravitational perturbations are transmitted to the geosphere through the acceleration derivative - kinematic jerk, and i.e. they have a phase shift relative to the acceleration graph. For this reason, there is a time shift between the moment of alignment of celestial bodies and the manifestation of natural events with the advance or lag of natural phenomena. (Confirmed by the experiments of A. F. Pugach during solar and lunar eclipses, and the covering of Venus by the Moon). This time shift depends on the natural phenomenon size and can comprise intervals from minutes to several weeks.

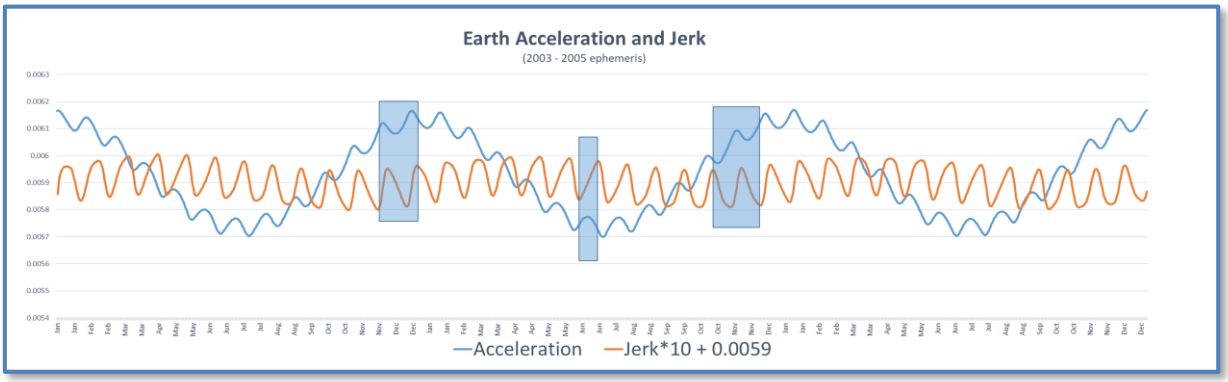

Figure 1. Phase shift between acceleration and kinematic jerk.

3.4. The more powerful natural phenomena correspond to alignment of several celestial bodies, several alignment lines, and a closer angular separations.

We claim that the celestial bodies alignments noted above, in all their diversity, are integral effects accompanying all significant natural phenomena. More powerful natural phenomena manifestations correspond to simultaneous alignment of several celestial bodies along the same line, the presence of several alignment lines, as well as a closer angular separation from astronomical conjunctions, or oppositions.

3.5. Examples of celestial bodies' alignments associated with major natural phenomena.

Figure 4 shows alignments of the celestial bodies for a number of large eruptions of Etna. For ancient eruptions, an unknown date was selected according to the nearest extreme alignment of the celestial bodies.

The Moon and the inner planets move around the celestial sphere faster than other bodies, and under certain circumstances can cause fast-flowing paroxysms of Etna, coinciding with the moments of alignment of the Moon and the planets in terms of the start time and duration, within an accuracy of fractions of hours (Table 2).

Table 2. Etna paroxysms associated with the celestial bodies' alignments.

Dates	Alignment	Reference
10.05.2008	Earth-Moon-Mars	[2]
29.03.2007	Earth-Moon-Saturn	[3]
29.04.2007	Earth-Mars-Uranus	[3]
15.11.2011	Earth-Mercury-Venus	[1]
18.03.2012	Earth-Mercury-Uranus	[1]
04.12.2015	Earth-Moon-Jupiter	[4]
12.01.2011	Mercury-Earth-M35	[5]
19-23.02.2013	Earth-Sun-Neptune	[5]
27-02-2017	Earth-Mars-Uranus	[6]
13-15.04.2017	Earth-Sun-Uranus	[6]
19-21.04.2017	Earth-Mercury-Sun	[6]

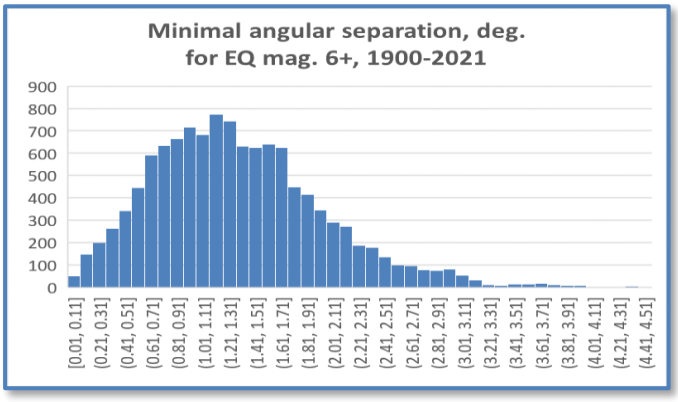

Figure 2. Minimal angular separation for EQ mag. 6+, 1900 – 2021.

We calculated the angular separations between the celestial bodies (Figure 2) relative to each other, and relative to 13 stellar objects at the moments of 11,726 earthquakes of magnitude 6+, filtered and displayed them on the graph (Figure 3) to identify a possible spatial grouping. A similar procedure was performed for three series of randomly generated dates. We were not able to identify significant statistical differences, or a special spatial grouping of the natural series in comparison with random ones. The obvious reason is that the alignment of celestial bodies is just a precondition, i.e. a prerequisite for the manifestation of an event, just as the presence of clouds is a necessary condition for rain, but not every cloud rains. The sum of the gravitational perturbation vectors takes extreme values only in the case of their corresponding mutual orientation, which cannot be detected by statistical analysis. The second reason is the presence of a time lag of variable length between the alignment of celestial bodies and the event (discussed below). To confirm the statistical dependence, an analysis of the calculated values of gravitational perturbations is required.

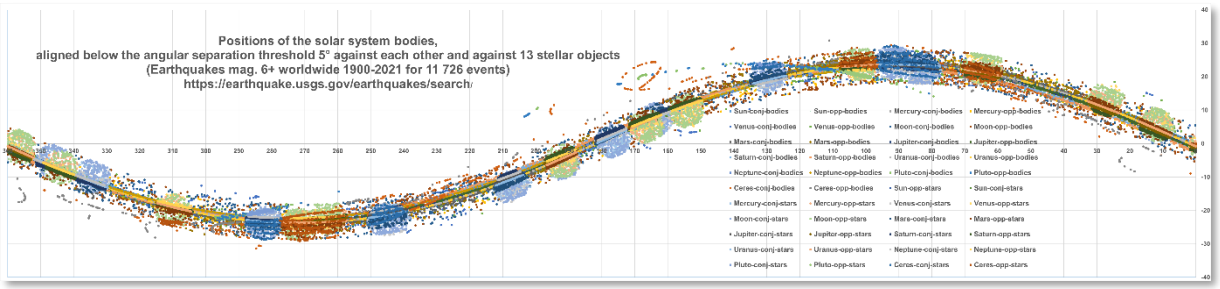

Figure 3. Positions of the solar system bodies aligned below the angular separation threshold 5°, for earthquakes mag. 6 + 1900-2021, 11 726 events (RA°, DEC).

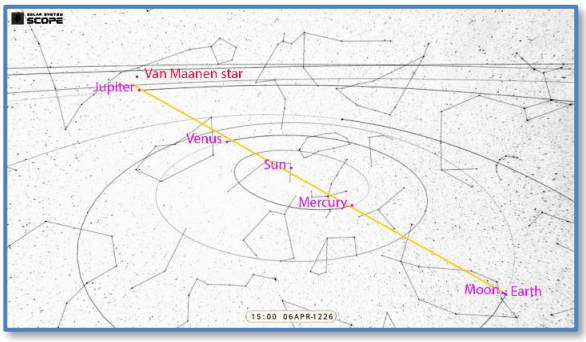

1226 B.C. The first historically confirmed eruption of Etna.

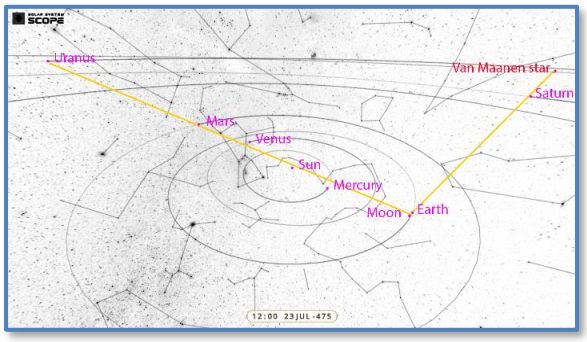

475 B.C. Mount Etna eruption (according to Pindar and Aeschylus).

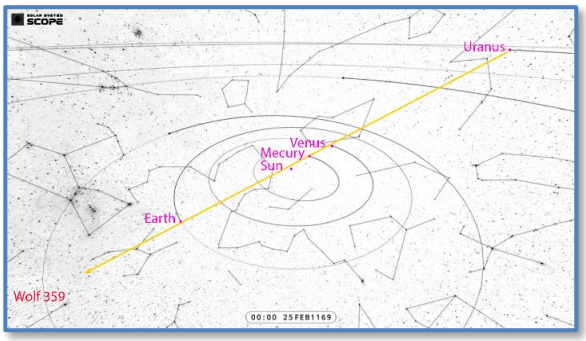

1169 A.D. A powerful eruption of Etna and an earthquake.

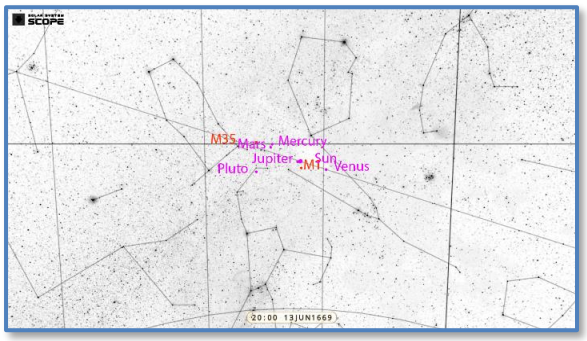

13 June 1669. The eruption of Etna changed the contour of the coast.

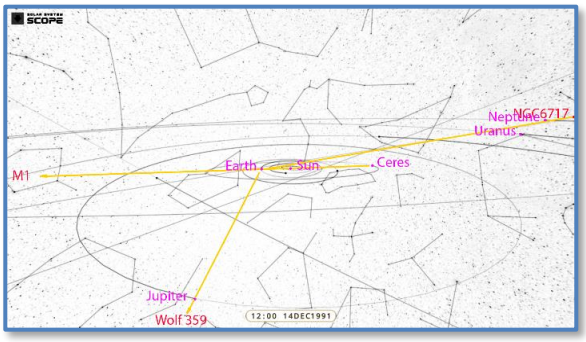

14 December 1991. One of the largest eruptions of Etna.

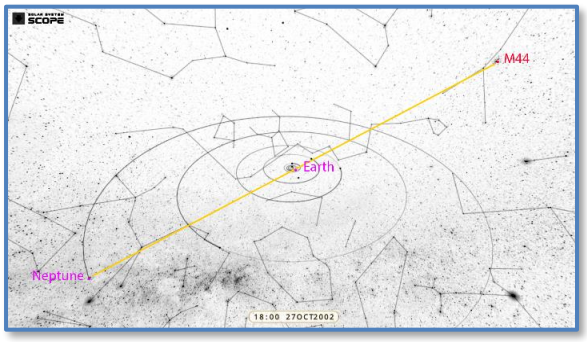

13 June 2001. Etna volcanic activity.

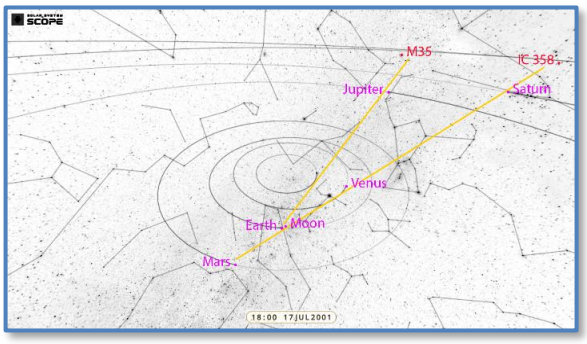

17 July 2001. Etna volcanic activity.

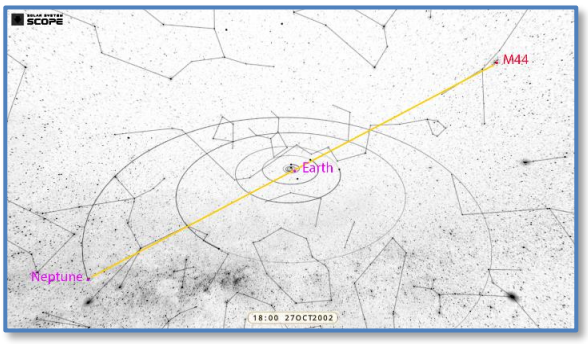

27 October 2002. Etna volcanic activity.

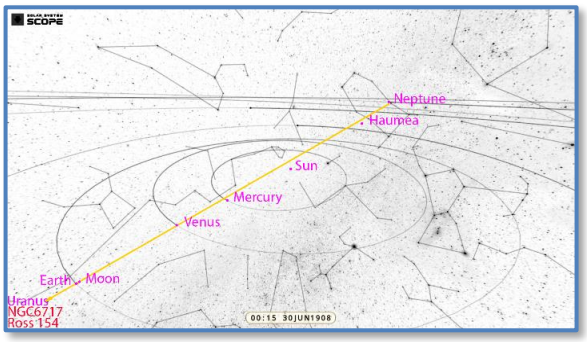

30 June 1908. Tunguska Event, Russia (volcanic version).

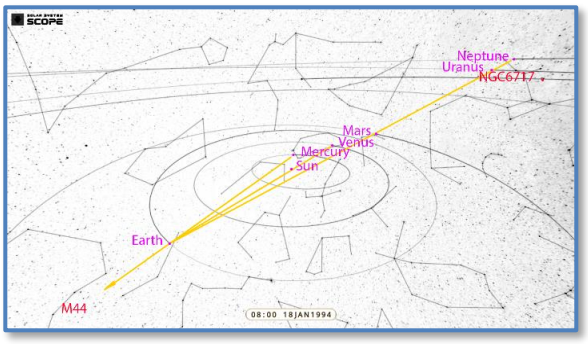

18 January 1994. Event in Cando, Spain (similar to Tunguska).

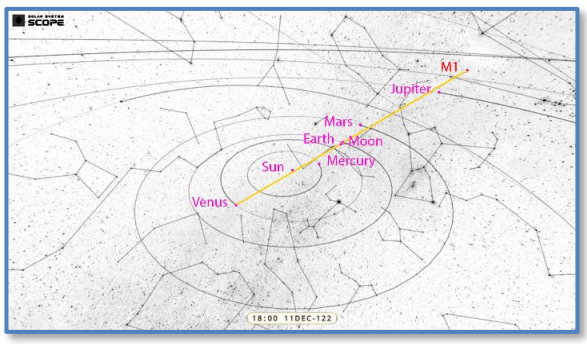

122 B.C. Etna almost wiped out the city of Catania.

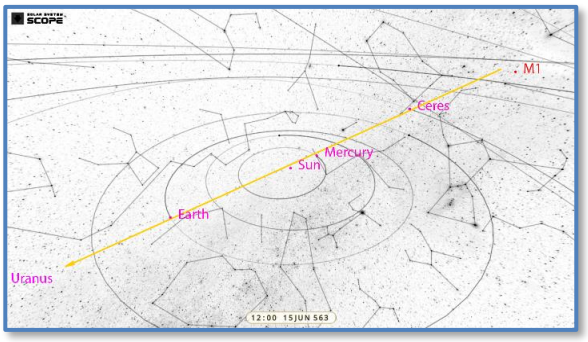

563 A.D. Landslide on Mount Taurendum, caused tsunami on Lake Geneva.

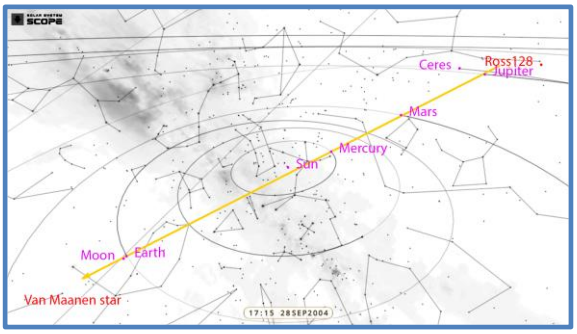

28 September 2004. Parkfield earthquake.

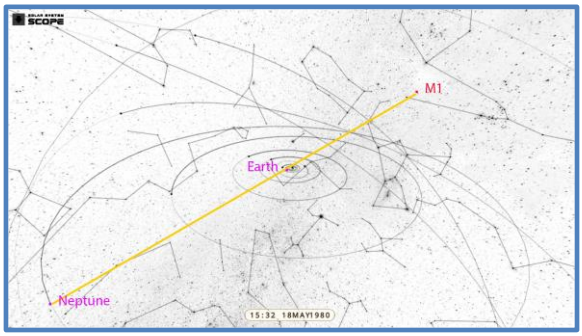

18 May 1980. Eruption of Mount St. Helens.

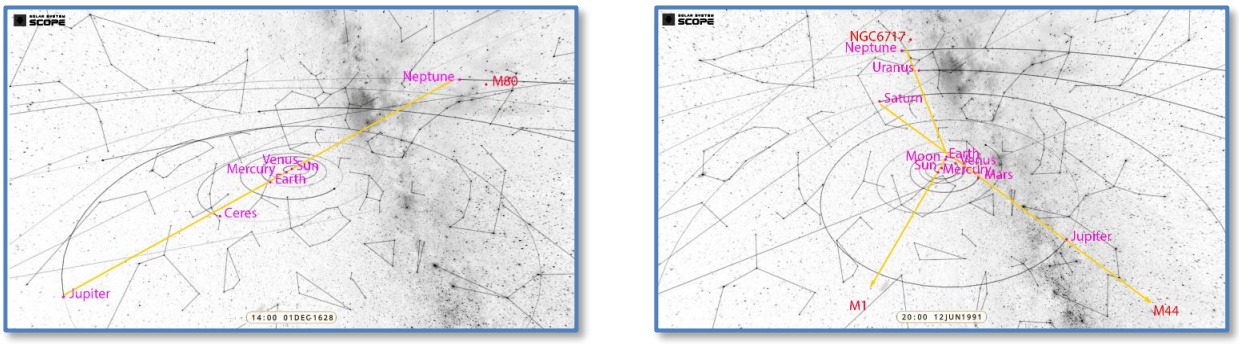

1628 B.C Minoan Eruption (Santorini). 12 June 1991. Pinatubo eruption.

Figure 4. Examples of celestial bodies' alignments, associated with the major natural phenomena.

4. Bidirectional Pushing Gravitation model (BPG)

The conclusions obtained as a result of the analysis of celestial bodies' positions accompanying natural events on Earth do not allow us to propose an appropriate mechanism operating within the framework of the standard cosmological model. Our approach, discussed below, assumes the interpretation of the observed relativistic phenomena of GRT, such as the deflection of geodesic lines near celestial bodies and the Shapiro delay, as gravitationally effective, within the framework of the extension of the law of universal gravitation. The employment of alternative cosmology is dictated by the need to use the bidirectional action of gravitational forces in a closed stationary universe, that is unacceptable in the standard cosmological model, as well as the effect of the "lens of the universe", which ensures the participation of the entire celestial sphere in the gravitational interaction of bodies as an intermediary, without which this interaction cannot occur. The parametrized post-Newtonian formalism (PPN), usually employed for the analysis of alternative theories, is not applicable here, since with the introduction of the apparent gravitational mass, the Einstein equivalence principle for distant bodies is violated.

4.1. Effective gravitational self-lensing and apparent gravitational mass

As is known, the problem of "dark matter", which has appeared since the time of Zwicky's observations, arises due to the discrepancy between the velocities of the circular motion of stars in galaxies and the Kepler curve equation.

$$V(D)=\sqrt{\frac{GM_g}{D}}. \qquad (2)$$

Here, $\mathbf{M_g}$ – mass of the galaxy, and $\boldsymbol{D}$ – distance to star, and the speeds of the stars decrease proportionally $\sqrt{1/D}$. Instead, the rotation curves of galaxies have plateaus. Thus, to get a plateau on the rotation curves of galaxies, without reducing the velocities of stars, an increase is required in $\boldsymbol{M_g}$ proportionally to D.

Precisely this kind of dependence A. Einstein mentioned in his famous work dated 1936, "Lens-like action of a star by the deviation of light in the gravitational field". He emphasized that the phenomenon of gravitational lensing obeys increase in proportion to $\sqrt{D}$, which in our opinion indicates about the possible participation of this phenomenon in the formation of rotation curves of galaxies

The relativistic deflection of the hyperbolic trajectory of geodesic lines near the solar disk comprises half of the magnitude of this deflection calculated for distant stars (~1.75"). Such a deflection indicates the presence of an observational increase in the geometric properties of the celestial body, in particular, the apparent radius of the Sun, or of any other celestial body. This effect called gravitational self-lensing [14], [15] and considered exclusively as an insignificant optical phenomenon, limited by the laws of

geometric optics. However, we believe that in the case of gravitational lensing, in contrast to geometric optics, **the solid angle occupied by the enlarged object on the celestial sphere changes**. As a result, the apparent increase in the geometric properties (including the apparent gravitational radius of the body), under gravitational lensing becomes effective, and violates the law of inverse squares, which lies in the basis of the law of universal gravitation. Thus, the law of universal gravity ceases to be the limiting case for GRT and requires adjustment.

In order to highlight the parameters and constants of the new model, we will mark them with a subscript #.

We introduce the concept of an *apparent gravitational mass,* $M_{\#} = M(1+C_{\#} \cdot D)$, which ceases to be invariant and depends on the integral mass self-lensing coefficient of the celestial body $C_{\#}$, determined by its compactness, as well as on the distance D to the observer. The notion of the *apparent gravitational mass* significantly increases the long-range action of gravitation for compact masses or celestial bodies having a compact core and a large integral coefficient of gravitational self-lensing of the mass. This makes it possible to explain the rotation curves of galaxies by the presence of a highly compact central mass without involving the concept of dark matter. The compactness of the central mass in galaxies corresponds to the size of their turning radius, which is determined by the balance of centrifugal forces and gravitational forces. Another task of the introduced concept of the *apparent gravitational mass* is the formation of a distributed repulsive potential of the celestial sphere, as a whole.

In this regard, the question arises on the applicability of Bertrand's theorem [13], which protect the law of universal gravitation from encroachments. J. L. F. Bertrand proved that the law of force, which depends only on distance, and makes its point of application move along an algebraic curve, could be either Hooke's law or the law of universal gravitation. The bodies moving in closed orbits according to the law of universal gravitation must follow elliptical orbits.

4.2. Bertrand's theorem is not applicable in a curved space

Generally accepted that violations of the law of universal gravitation can be determined by means of measuring parameters of the orbits using the radar method. However, the length in the international system of units defined basing on the speed of light. According to A. Einstein, the speed of light in a gravitational field decreases due to gravitational time dilation. If we deal with the additional gravity, not caused by the appearance of a third mass between two interacting ones, but due to the very law of gravity, then we must take into account such additional time dilation in radar or laser measurements of the orbits.

Bertrand's theorem applies to Euclidean coordinates. If the law of gravity contains unknown additional terms, depending on the distance, which affect the time dilation in gravitational field, then by affecting the speed of light, this will change the gradation of the distance scale for radar measurements, and we will deal with curved coordinates (without knowing this). Thus, the radar method fundamentally does not allow detecting the presence of additional gravitation in the law. The assumed violations of the ellipticity of orbits for the modified law of gravity canceled out by the corresponding time dilation in gravitational field. This also applies to checking the ellipticity of the orbits for stars orbiting the center of galaxy in the image plane. For a curved space, Bertrand's theorem is inapplicable.

4.3. The "lens of the universe" effect and bidirectional action of forces in a stationary closed universe

We employ an alternative cosmological model for a stationary closed universe without inflation. The world space represented by a three-dimensional surface of the hypersphere S^3 with a radius of ~1500 Mpc. Instead of the classical attraction, forces of gravitational repulsion act instantly between the gravitating body and the test mass, both in the forward and in the opposite direction (since the space of the universe, which is a topological manifold, is closed). These repulsive forces are equal in magnitude and mutually compensated. However, in the forward direction, the gravitating mass also shields part of the celestial sphere, blocking the action of repulsive forces applied to the test mass from other distant celestial bodies. Due to the shielding, the compensation for the repulsive forces violated, and attraction

emerges. Actually, this is not an attraction of the test body to the gravitating mass, but pushing from the side of the celestial sphere.

Compared to Newtonian gravity, the agents of the interaction change, as well as the direction and number of forces. Due to increase in the range of action for gravitation, and the presence of remote compact masses distributed throughout the entire celestial sphere, the celestial sphere, which has a high gravitational repulsive potential, distributed over its area, becomes the third agent, mediator in the gravitational interaction, without which it cannot occur. This potential pertains to an indefinite set of distant massive bodies in the universe, the long-range gravitation of which is due to the self-lensing of their gravitational mass with distance, as well as with an apparent (but effective) cosmological scaling, due to "lens of the universe" effect (mentioned by J. Wheeler in "Gravitation" [12]).

The closed space of the hypersphere surface (topological manifold S^3) pertains apparent projective scale magnification. For the convenience of insight of the apparent scale magnification in the space of positive curvature, one can lower the dimension of space and consider the surface of the sphere S2 (the Earth's surface). In the azimuthal equidistant projection (Postel's projection), often used to select directions for long-distance radio communication (Figure 6), for an operator located at the pole, an object removed to the equator will have an apparent scale increased in $\boldsymbol{\pi/2}$ times, and at the antipodal point, as well as, when closing the circle, the apparent scale increases asymptotically (Figure 5). It is important to understand that the projective increase is applied to solid angles (because the radius and area of the distant full sphere are reduced). It causes a red shift due to the apparent increase in the size of any cosmologically distant oscillators. This also means that the existence of a time rate declaration for cosmologically distant objects (Just imagine the atomic frequency standards of aliens :).

The increase in redshift with distance due to the lens of the universe effect offers an alternative explanation for the Olbers' paradox instead of the Doppler's effect and eliminates the need for an inflationary model. The entire closed universe acquires the properties of a cosmological black hole, wherein it generates blackbody radiation, interpreted in the standard cosmological model as a cosmic microwave background radiation.

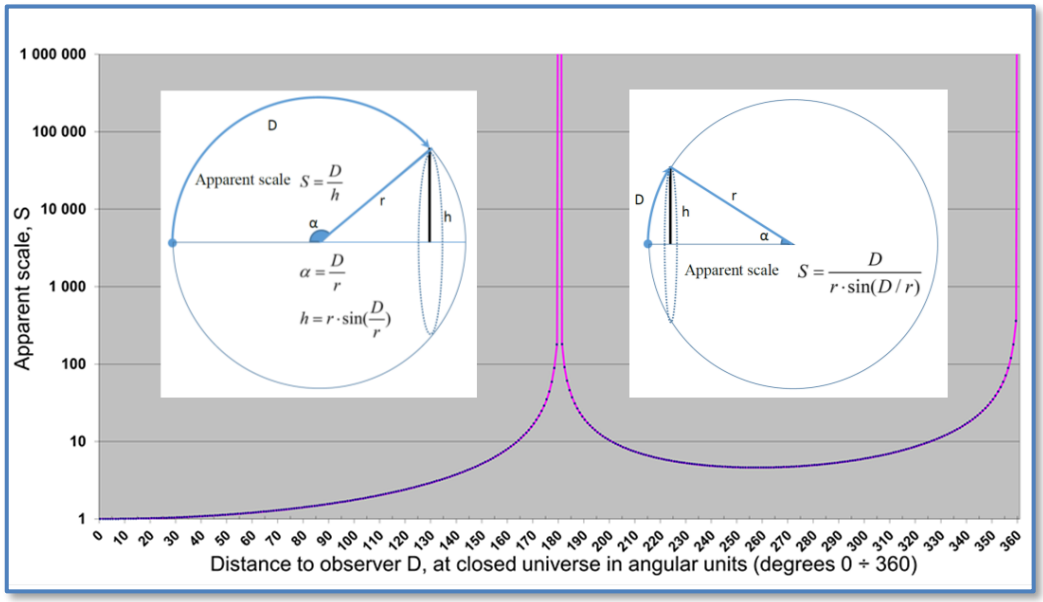

Figure 5. Apparent scale in a stationary closed universe (hypersphere S^3).

In the antipodal zone of the universe, persists an asymptotic increase of the projective scale, causing a strong frequency shift. Thus, with a projective magnification in 10^7 times, the frequencies of the visible

range are shifted to the band of radio frequencies of the decimeter range. Accordingly, the apparent increased size of radio galaxies, is taken for their own size.

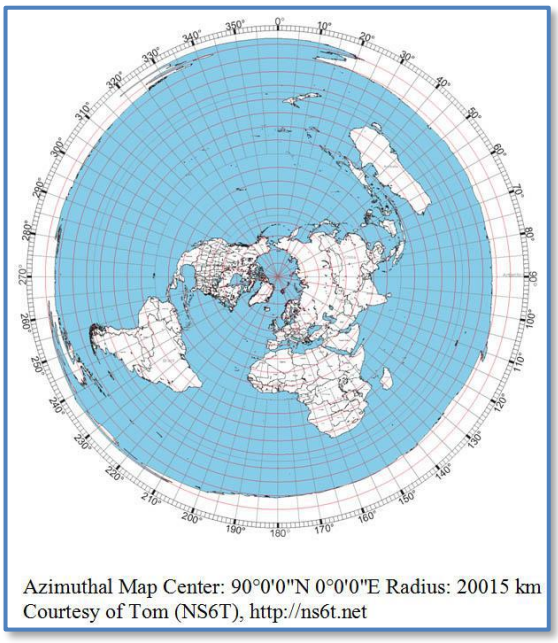

Figure 6. Azimuthal map projection.

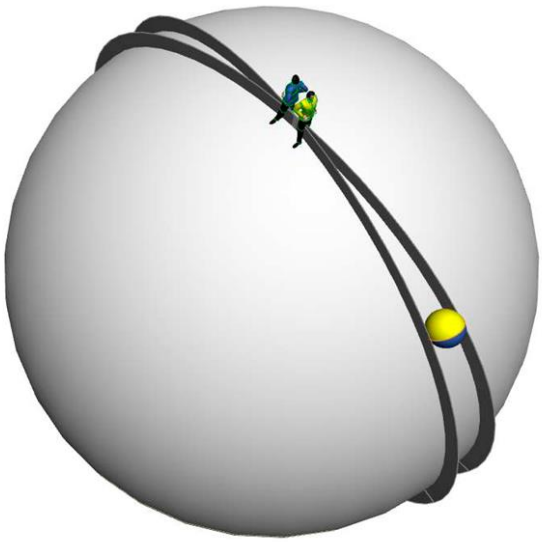

Figure 7. Bidirectional projection in a closed manifold S^2.

If the light propagated instantly, then an observer viewing the Moon in the forward direction could try to "observe" its reverse side in the opposite direction (through the Earth), moreover, of the same angular size, but upside down. However, the asymptotic growth of the projective scale at such a distance appropriately shifts the frequencies of electromagnetic oscillations, which makes this task unsolvable. The geometric relations in a closed space shown in the Figure 7 demonstrate possibility of applying the inverse square law in two opposite directions simultaneously, and give rise to consider the proposed mechanism of action for the compensated pushing gravitational forces plausible.

The lens of the universe effect requires an adjustment of the photometric distance modulus equation (Figure 8, see also [9]). At the same time, a kink appears on the graph, the position of which depends on the presupposed radius of the hypersphere of the universe. **For r = 1500 Mpc**, the beginning of the accelerated darkening of supernovae SN1A (the kink at the graph) falls on the values of the stellar magnitude **m = 21 ÷ 22**, which allows us to choose the radius value and offer an alternative interpretation for the "accelerated expansion of the universe".

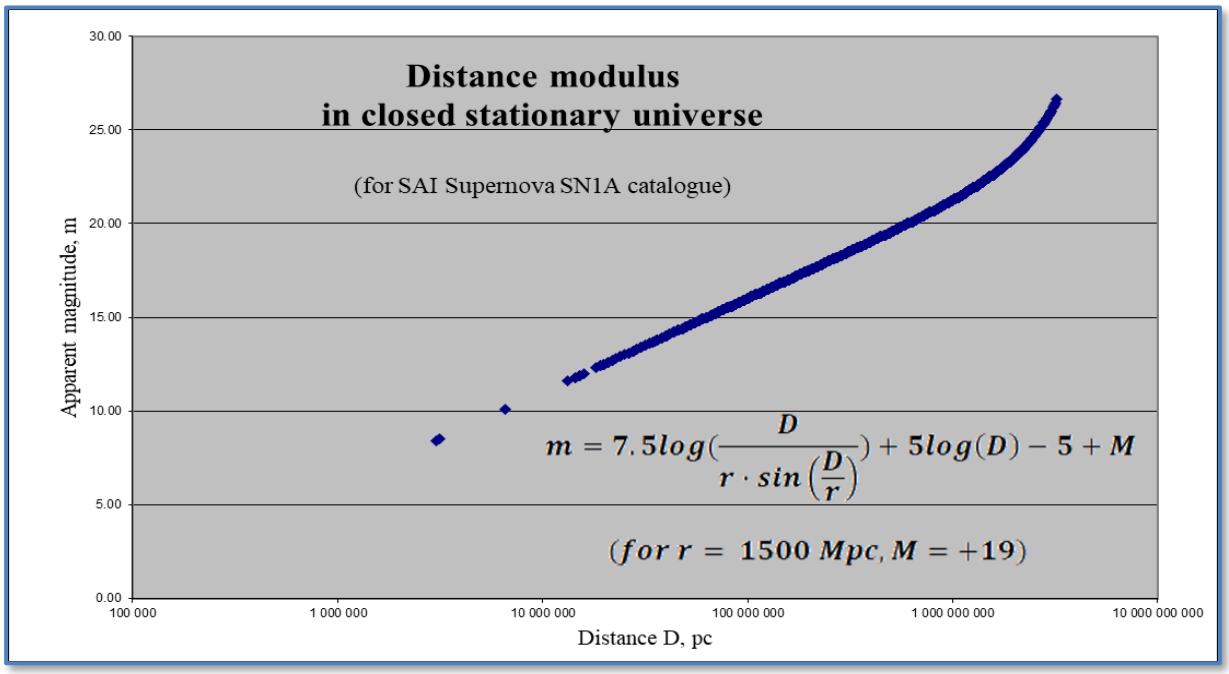

Figure 8. Distance modulus in the stationary closed universe.

4.4. The phenomenon of gravitation is caused by the effect of shielding the celestial sphere repulsion

The question arises: "What is the magnitude of the specific strength of the gravitational repulsive field of the celestial sphere $\mathbf{E}_{\#}$"? For calculations, we will use the following dependencies:

Gravitational field strength: $E=GM/D^2$. Gravitational radius: $r_g=2GM/c^2$. Solid angle occupied by a circle of radius **r**: $\Omega=\pi r^2/D^2$. Strength of the gravitational field per the solid angle, shielded by the mass on the celestial sphere $E=\Omega E_{\#}$.

After substitutions and transformations, we get**:** $E_{\#}=E/\Omega=GM/(\pi r^2)$. If we define the radius of the circle of the gravitational shadow as $r_{\#}=\sqrt{r_g/\pi}$ **,** then we get:

$$E_{\#}=\frac{c^2}{2}\ (\text{m/s}^2 \text{ per one steradian}). \quad (3)$$

To get rid of the big figures, calculated for a solid angle of 1 sq. second, this value should be divided by $\mathbf{(180 \times 60 \times 60/\pi)^2}$ sq. seconds in one steradian.

Thus, it is possible to propose a universal constant for magnitude of the specific strength of gravitational repulsive field of celestial sphere, applied to the gravitational shadow of the mass, as a circle with radius $r_{\#}=\left(r_g/\pi\right)^{1/2}$, acting in a solid angle:

$$E_{\#}=1056236.4335137\ (\text{m/s}^2 \text{ per one sq. second of a solid angle}).$$

For an observer on the Earth's surface $(D=6\ 371\ 000\ \text{m})$, the Earth's gravitational radius $\left(r_g=0.008857538\ m\right)$ occupies a solid angle $\Omega=2.18221632\text{E-}16$, which comprises $9.28427648\text{E-}06$ sq. seconds, thus, the gravitational field strength equals:

$$E=\Omega \cdot E_{\#}=9.28427648\text{E-}06 \cdot 1.0562364335137\text{E+}06=9.81\ \text{m/s}^2.$$

We argue that the very phenomenon of gravity exists due to the effect of shielding the celestial sphere. It is due to this mechanism the inverse square law operates in the gravitational interaction. This case, owing to the presence of a distributed repulsing gravitational potential of the celestial sphere, is radically different from the intended mass shielding effect for two bodies, where strict limits established in the experiments.

4.5. Parameterization of the model. The integral coefficient of gravitational self-lensing of mass.
The angle of the relativistic deflection, and the corresponding magnification coefficient **k (d)** for a thin cylindrical layer is determined by the value of the impact parameter d and the fraction of the body mass (having gravitational radius $\mathbf{r_g}$) located inside the impact parameter.

$$k(d) = 1 + \frac{r_g(d) \cdot D}{d^2}. \tag{4}$$

The total value of the gravitational self-lensing coefficient of the mass $\boldsymbol{C_\#}$ of a celestial body can be obtained based on the radial density distribution by means of layer-by-layer integration over a changing impact parameter. For example, the self-lensing coefficient of the Sun obtained by numerical integration for the standard solar model is 1.18% increase of the apparent gravitational mass per 1 AU. For compact celestial bodies with a high average density, the self-lensing coefficient will be high, and the range of their gravity will significantly increase.

For compact stars, such as red dwarfs, white dwarfs, neutron stars, etc., the calculation of self-lensing coefficients can be performed on the basis of the accepted polytropic model for corresponding classes of stars, their known mass and radius. It should be borne in mind that many theoretical models in astrophysics, including data on the masses and radii of stars, as well as on the internal structure of planets, require their verification, and for clusters and other galaxies may be completely absent.

The most reliable way to parameterize the proposed model will be the parameters fitting technique by solving a redundant system of equations. Such a system of equations can be compiled using data on the manifestations of natural events that have a time reference, for selecting the amplitudes of gravitational perturbation vectors induced by corresponding sources of gravity, with known orts of directions to these sources.

4.6. Induction of gravitational perturbations in geosphere due to alignment of celestial bodies
Celestial bodies are affected by compensated powerful forces of repulsive gravity from other celestial bodies distributed over the celestial sphere. However, the repulsive potential of the celestial sphere is not uniform. Outside the solar system, at various distances, there are many compact and massive bodies, as well as their clusters, the repulsive (and at the same time, compensated) gravitation of which has significant values. The inhomogeneity of gravitational potential of the celestial sphere is the main reason that does not allow obtaining exact value of the gravitational constant in different experiments.

The bodies of the solar system, approaching the line of interaction of a distant gravitating mass and a test body, act as gravitational lenses, causing relativistic deflection of the powerful repulsive forces applied to the test body. This deflection induces a vector of gravitational perturbations at the test body, directed orthogonally to the repulsive force.

All the bodies of the solar system, moving along the celestial sphere, are involved in formation of the total vector of disturbances. The impulse to the test body transmitted not by the vectors of total perturbation of the gravitational field strength (accelerations), but by its derivative, known as kinematic jerk.

The relativistic deviation of the direction to the source of gravity also causes an apparent increase in the distance to the source OS' in comparison with OS (Figure 9), as the impact parameter decreases (for sources located further than the deflecting mass) and a corresponding change in the strength of the gravitational field. The Shapiro effect, known as gravitational signal delay, causes similar effective increase in the apparent distance to the source and a change in the field strength. As a result, motion of the deflecting mass breaks compensation of the repulsive forces and creates a kinematic jerk.

The most effective impact on free masses will take place along the plane of horizon of the observer (rotating in space with the Earth). Thus, it is required to calculate the projection of the estimated vector of gravitational disturbances (hodograph of jerks in time window) onto the plane of horizon of the observer. If we integrate the obtained vector field of disturbances in the time window, we can obtain the impulse of force transmitted to the certain geophysical object.

The impact of small gravitational perturbations' (non-tidal variations of plumb line deviation) on the free surface of a large area of liquids (e.g., the sea surface, magma layers of different densities) can cause extreme waves and seiches.

4.7. Relativistic gravitational deflection of geodetic lines

The influence of relativistic gravitational deflection of light by celestial bodies of the solar system on the accuracy of astrometric measurements was studied in detail in the paper by Slava Turyshev and the references given therein [8]. In preparation for the cancelled mission of the space interferometer (SIM), a conclusion is made about the significant contribution to the astrometric observations of the microsecond accuracy of the relativistic gravitational deflection by the monopole gravitational components of all large celestial bodies of the solar system, as well as about the significant value of the quadrupole components of the fields of outer planets of the Solar system. The monopole deflection depends only on the mass of the gravitational lens and the impact parameter (Figure 9).

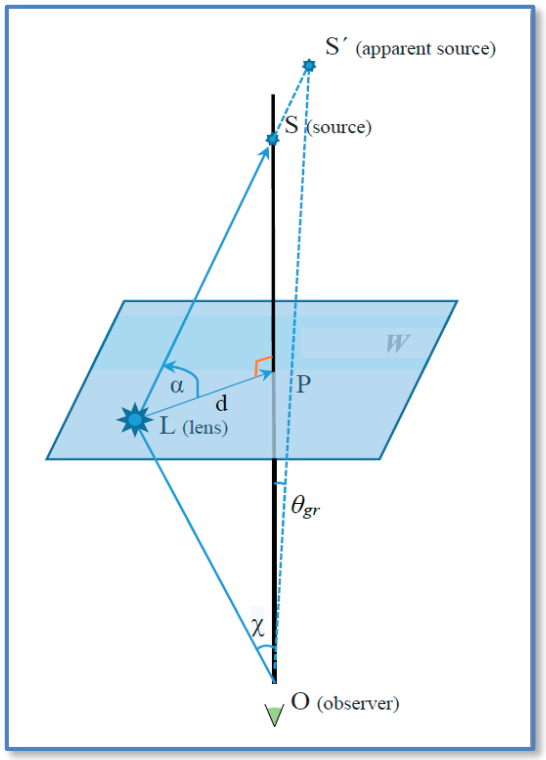

Gravitational deflection angle θ_{gr} for distant stars depends upon the impact parameter d [8].

$$\theta_{gr} = \frac{4GM}{c^2 d} \cdot \frac{1+\cos\chi}{2}. \quad (5)$$

For the Solar system bodies, **including sources located closer to observer, than a gravitational lens** (deflecting body):

$$\theta_{gr}(\alpha) = \frac{4GM}{c^2 d} \cdot \frac{1+\cos(\alpha)}{2} \cdot (1+\sin(\alpha)); \quad (6)$$

$$-\frac{\pi}{2} \le \alpha \le +\frac{\pi}{2}.$$

Or, for the convenience of computing:

$$\theta_{gr}(\beta) = \frac{4GM}{c^2 d} \cdot \frac{1+\cos(\alpha)}{2} \cdot (1+\cos(\beta)); \quad (7)$$

$$0 \le \beta \le \pi.$$

Apparent distance to source OS:

$$D_{s'} = D_S \frac{\sin(\beta)}{\sin(\theta_{gr})}. \quad (8)$$

Figure 9. The gravitational deflection geometry.

Celestial bodies of the Solar system at small angular separations from other celestial bodies exert a mutual gravitational deflection, and thus can expand the zone of their influence, cascading the transmission of induced gravitational deflection through other celestial bodies acting as gravitational lenses.

When calculating the quadrupole deflection, the second zonal harmonic of the geopotential J2, determined by the polar compression of the planet, will be of significant importance. The corresponding formalism for calculating quadrupole deflection is given in [8].

4.8. The speed of gravity, subatomic structure of matter and ejection of plasma by gravitational field

In the Bidirectional Repulsive Gravitation (BPG) model, the compensated gravitational forces affect instantly, both in the forward and in the opposite direction. This approach requires a justification of the instantaneous action mechanics. We do not use the classical ideas about the necessity of force-carrying particles considered in the early models of Le Sage [11]. The mutual repulsion of masses is a manifestation of the natural property of matter particles to occupy free space. This is simply a choice of the direction of movement due to the collective behavior of matter particles, interpreted as forces. This property is clearly manifested in the behavior of gases, as well as liquids in weightlessness. The behavior of solids obeys more complex laws, which are also implemented in the fundamental structure of matter.

The BPG model is based on the idea that the world space is filled with a medium that transmits interactions and has a limit of fragmentation corresponding to the minimum Planck length ($L_{pl} = 10^{-33}$ cm). Such a property of the medium inevitably means the impossibility of existence of lengths that are not multiples of L_{pl}, and, consequently, the need for quantization of the volume. In fact, such a medium acquires the properties of discrete (cellular) space. The shape of the volume quantum should correspond to the principle of the least action when moving to an adjacent cell. It is proved that a face-centered cubic lattice (FCC-lattice) is the densest regular packing of spheres in three-dimensional space and has the largest number of symmetries. The Voronoi-Delaunay cell for the FCC lattice has the shape of a rhombic dodecahedron. Thus, we can talk about filling the world space with a discrete medium, portions of which have the properties of a perfectly rigid bodies. The only possible metaphor for movement in a dense spatial packing of rhombic dodecahedra can only be the permutation of portions of the medium into neighboring vacant cells of the FCC lattice. This looks similar to the" Game of 15" (Slider-game) rules, but the role of square chips on the plane is performed by rhombic dodecahedra in the three-dimensional space.

Aristotle and the ancient atomists established that a discrete space has three fundamental properties - *isotachy*, *kekinema* and *renovation* [10], [24]. At the subatomic level, the structure of matter can be represented as a three-dimensional cellular automation on a FCC lattice (Figure 10), in which there is a permutation of permanently existing elements of the medium, endowed with the fundamental property of occupying vacant cells of space, and at the same time, competitively implementing this property. In a discrete space, there are only two speeds, 0 (invariantly stationary crystalline ether) and the "speed of light" - the only possible speed of moving elements of the medium to the neighboring cell of the lattice. The entire spectrum of velocities observed in the macrocosm is due to the movement of ensembles of elements, where each element moves with a “speed of light”.

The fact that the speed of light is invariant in different reference frames is due to the principle of the *isotachy* of discrete space and the existence of an invariantly stationary ether.

Each cell of the FCC lattice has 12 adjacent faces and 6 adjacent vertices with neighboring cells. If in the" Game of 15 " for one vacant cell, four adjacent chips can competitively strive to occupy it, then on the HCC grid, on the contrary, several vacant cells are required for a single (movable) element in a dense spatial packing. One will need at least three vacant cells adjacent to the three-sided vertex of the rhombic dodecahedron, or five vacant cells adjacent to the four-sided vertex. A complex competitive unidirectional dynamics that emerge generating persistent ensembles of elements, and implementing mechanics of the "arrow of time". As the analysis has shown, in order to build an algorithm for competitive occupation of free cells, it will inevitably be necessary to allow the possibility of accumulation of several elements of the medium in one cell of the FCC-lattice. As a result, we can consider a kind of the weird quantum potential dynamics according to the rules of the cellular automaton. In this model, subatomic particles of matter or energy correspond to vacancies, or to cells with fewer elements of the medium in one cell of the FCC lattice.

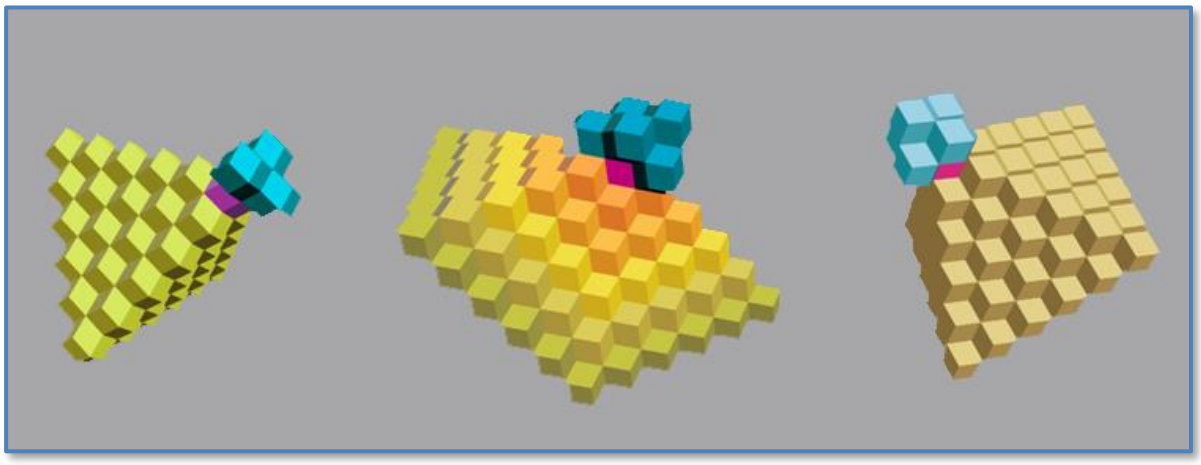

Figure 10. Cellular automata using Planck-size FCC-lattice.

4.9. On the closure of a three-dimensional space

The space of the universe is represented to an observer immersed in this space as a closed three-dimensional manifold - the surface of the hypersphere S^3 (in fact, it is a pseudo-hypersphere). Such an observer draws conclusions by evaluating the directions of radiation fluxes and measuring distances using the radar method. Our attempts to construct a model of the closure of the spatial packing of rhombic dodecahedra in the 4th dimension, just as it is done for a hypercube in the architecture of supercomputers by topologically gluing its faces, were unsuccessful, since all the external surfaces of the spatial packing of rhombic dodecahedra are oriented, and do not allow gluing with another external surface. However, a virtual observer located outside the universe will not detect the fourth spatial dimension. For an external observer the trajectories of light rays will be represented as polylines of Planck length segments in Euclidean space, bending towards the cells of space with a lower density of the medium, a kind of a cosmological black-hole in 3D-space.

The instantaneous "impact" of gravitational forces in the described subatomic structure is provided through the contact of neighboring portions of the medium having the properties of absolutely solid bodies. However, along with the *instantaneous impact*, there exists a *contact interaction* in the model under consideration, due to the movement of ensembles of elements, the speed of which corresponds to the property of the *isotachy* of discrete space, and limited by the ”speed of light". The described subatomic structure allows the construction of a computer simulation that excludes participation of an immersed observer. A detailed description of the applied space model is beyond the scope of this publication.

4.10. Why hasn't everything collapsed yet?

If the repulsive forces are compensated, and the celestial sphere pushes all the masses to each other, as a result, a collapse should occur. What mechanics resists the pushing of bodies? As noted above, the "lens of the universe" effect causes an asymptotic increase in the observed geometric characteristics of bodies when the circle is closed in the opposite direction. In addition to the apparent sizes of bodies, the sizes of any electromagnetic oscillators, the gravitational radii of bodies, also the observed value of the minimum Planck length increases asymptotically. A quantum threshold arises that restricts transfer of gravitational repulsion forces to ensembles of subatomic elements whose physical size happen to be less than the apparent size of the Planck length. Thus, compensation of the repulsive forces is violated. The plasma is pushed out by the gravitational field [19]. This effect can manifest itself in heating of the solar corona and ionosphere, determine the position of ionopause of the solar system planets, the dynamics of comets' ion tails, astrophysical jets.

5. Conclusions

To give a final answer to the question in the title of the report will be possible only after calculating the gravitational perturbations in accordance with the proposed model. At the moment, we are at the preliminary stage of research and invite interested specialists.

The causal relationship between high-energy natural phenomena and assumed or registered gravitational disturbances accompanying them is interpreted ambiguously. Free masses begin to move when plumb line deviations vary, and vice versa, with the movement of masses, deviations of plumb lines are changing. What is the cause and what is the effect? We have considered the hypothesis about the possibility of transmitting gravitational field perturbations from extraterrestrial masses, and we propose corresponding mechanics and model.

However, computational test of the hypothesis is required. To do this, it is necessary to perform a detailed parameterization of the model (section 4.5). This task will require an interdisciplinary approach of specialists in astrophysics and Earth sciences, performing substantial amount of calculations for selecting model parameters using computational methods, expanding the list of stellar objects, including those, not only near the ecliptic.

It would be possible to check out the model by measuring a spacecraft flight path disturbances of a spacecraft, planning (correction) of space missions for navigation in conditions of celestial bodies' alignments.

In addition to various applied problems in the geosphere (lithosphere, hydrosphere and atmosphere), the application of this model is possible in planetology (volcanism on planets and satellites of the Solar system), in solar physics (flares, CME), ionospheric studies.

The Discussion section will be submitted to the journal Frontiers in Earth Science.

References

[1] Bonaccorso A, Calvari S, Currenti G, Del Negro C, Ganci G, Linde A *et al* 2013 From source to surface: dynamics of Etna's lava fountains investigated by continuous strain, magnetic, ground and satellite thermal data. *Bull. Volcanol*. **75** 690

[2] Bonaccorso A, Cannata A, Corsaro RA, Di Grazia G, Gambino S, Greco F *et al* 2011 Multidisciplinary investigation on a lava fountain preceding a flank eruption: The 10 May 2008 Etna case. *Geochemistry, Geophysics, Geosystems* **12**

[3] Acocella V, Neri M, Behncke B, Bonforte A, Del Negro C and Ganci G 2016 Why Does a Mature Volcano Need New Vents? The Case of the New Southeast Crater at Etna. *Front. Earth Sci.* **4**

[4] Bonforte A, Cannavò F, Gambino S and Guglielmino F 2021 Combining High- and Low-Rate Geodetic Data Analysis for Unveiling Rapid Magma Transfer Feeding a Sequence of Violent Summit Paroxysms at Etna in Late 2015 *Appl. Sci.* **11** 4630

[5] Nunnari G 2021 *Earth Science Informatics* **14** 1121

[6] Viccaro M, Giuffrida M, Zuccarello F, Scandura M, Palano M and Gresta S 2019 Violent paroxysmal activity drives self-feeding magma replenishment at Mt. Etna. *Scientific Reports* **9**

[7] Sottili G, Martino S, Palladino DM, Paciello A and Bozzano F 2007 Effects of tidal stresses on volcanic activity at Mount Etna, Italy. *Geophys. Res. Lett*. **34**

[8] Turyshev V G 2009 Relativistic gravitational deflection of light and its impact on the modeling accuracy for the Space Interferometry Mission. *Astron. Lett*. **35** 215

[9] Heymann Y 2012 Redshift Adjustment to the Distance Modulus *Progress in Physics* **1**

[10] Korukhov V V and Sharypov O V 1995 On the possibility of combining the properties of invariant rest and relative motion on the basis of a new model of space with a minimum length (in Russian) *Philosophy of science* **1** 5

[11] Edwards M 2002 *Pushing Gravity. New perspectives on Le Sage's theory of gravitation.* (Montreal: Apeiron) pp 698-699

[12] Misner C W, Thorne K S, Wheeler J A and Chandrasekhar S 1973 *Gravitation* (San Francisco: Freeman) p 795

[13] Santos F C , Soares V and Tort A C 2011 An English translation of Bertrand's theorem *Latin American Journal of Physics Education* **5** 694
[14] Vargashkin V 2003 The phenomenon of gravitational self-lensing *Proceedings of International Scientific Meeting PIRT-2003* (Moscow: BMSTU press) p 82
[15] Prasanna A R and Ray S 2004 Self-Lensing effects for compact stars and their mass-radius relation *Mod. Phys. Lett.* **19** 2431
[16] Allais M 1999 The 'Allais Effect' and my experiments with the paraconical pendulum (1954-1960) *Memoir C-6083 prepared for NASA (Report)*
[17] Pugach A F 2018 Unexplained Temporal Effects Recorded by The Torsind at Syzygies *J. Adv. Phys.* **15** 5950
[18] Nugraha M G *et al* 2020 Anomalies of earth surface gravity field (g) during total lunar eclipse (TLE) on January 31 and July 28 2018 using video tracker analysis on pendulum harmonic motion. *J. Eng. Sci. Technol.* **15** 1001
http://jestec.taylors.edu.my/Vol%2015%20issue%202%20April%202020/15_2_20.pdf
[19] Dmitriev A L and Nikushchenko E M 2016 Expulsion of Plasma in A Gravitational Field. *Appl. Phys. Res*. **8** 38
[20] Wang Q, Yang X and Tang K 2001 Gravity anomaly during the Mohe total solar eclipse. *Sci. Bull. formerly: Chi. Sci. Bull*. **46** 1833
[21] Zhou S W and Huang B J 1992 Abnormalities of the time comparisons of atomic clocks during the solar eclipses. *Il Nuovo Cimento C*. **15** 133
[22] Barlik M, Bogusz J and Kaczorowski M 2009 Investigations on the field of gravity in Polish tidal laboratories *Reports on Geodesy* **86** 43
[23] Antonov Yu V and Antonova I Yu 2020 *Proceedings of Voronezh State University. Series: Geology* (Voronezh: Voronezh State University)
[24] Vyaltsev A N 1965 *Discrete space-time* (Moscow: Nauka publishers)
[25] https://volcano.si.edu/search_eruption.cfm
[26] https://earthquake.usgs.gov/earthquakes/search/
[27] https://www.astro.com/swisseph/swephinfo_e.htm
[28] https://www.alcyone.de/
[29] https://www.solarsystemscope.com/
[30] www.researchgate.net/profile/Ivan-Krasnyj/projects

Acknowledgements
The authors gratefully acknowledge the support of Professor Giuseppe Nunnari, Università degli Studi di Catania and Professor Innocenzo M. Pinto, University of Sannio at Benevento, Italy.